

# UNDERSTANDING THE CONNECTIONS BETWEEN GRAIN GROWTH AND FLUX EXPULSION IN LOW RRR NIOBIUM SRF CAVITIES\*

K. Howard<sup>†</sup>, Y.-K. Kim, University of Chicago, Chicago, IL, USA

D. Bafia, W. Dzierdzic-Misiewicz, Z. Sung, Fermi National Accelerator Laboratory, Batavia, IL, USA

## Abstract

The SRF community has shown that high temperature annealing can improve the flux expulsion of niobium cavities during cooldown. The required temperature will vary between cavities and different batches of material, typically around 800 °C and up to 1000 °C. However, for niobium with a low residual resistance ratio (RRR), even 1000 °C is not enough to improve its poor flux expulsion. The purpose of this study is to observe the grain growth behavior of low RRR niobium coupons subjected to high temperature annealing to identify the mechanism for improving flux expulsion in low RRR cavities. We anneal the low RRR material up to 1200 °C to understand the limits of flux expulsion performance. We observe that low RRR material experiences less grain growth than high RRR when annealed at the same temperature. We search for the limitations to grain growth in low RRR material and develop a diagnostic based on grain structure to determine the appropriate recipe for good flux expulsion. The results of this study have the potential to unlock a new understanding on SRF materials and enable the next generation of high  $Q_0$ /high gradient surface treatments.

## INTRODUCTION

As we approach the theoretical limits of niobium for superconducting radio-frequency (SRF) cavities, immense improvements in quality factor ( $Q_0$ ) and accelerating gradients have been possible though intentionally added impurities into the niobium surface [1]. Many SRF studies follow a "clean bulk dirty surface" technique by adding impurities to the surface layer of high purity niobium such as nitrogen through N-doping [2]. N-doped cavities are found to have a high sensitivity to trapped flux, so efficient flux expulsion has been critical for their implementation in accelerators [2–8].

During cavity testing, a fast cooldown is typically performed to prevent trapped magnetic flux [5–10]. In this process, there is a large thermal gradient across the cavity as it crosses through the superconducting transition temperature  $T_c$ . This allows for a sweeping phase transition to the Meissner state, where the depinning force is stronger than the attraction of the vortices to the pinning sites, and the flux is effectively expelled [7, 8]. As the cavity transitions to superconducting, the expulsion of flux from the cavity walls increases the magnetic field outside the cavity [8]. We observe a step change in the magnetic field, like in Fig. 1, which corresponds to the amount of flux expelled in this phase transition [8, 9].

\* FERMILAB-CONF-26-0331-TD

<sup>†</sup> khoward99@uchicago.edu

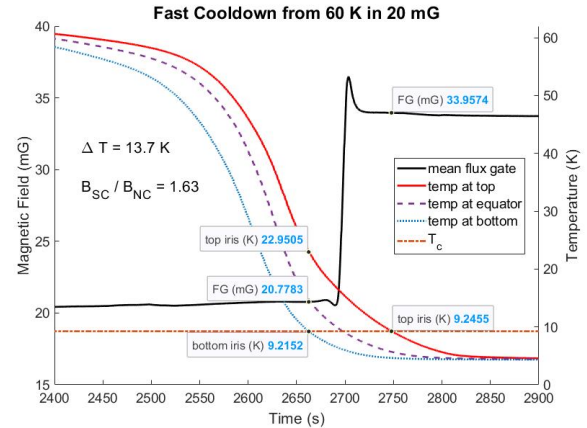


Figure 1: Fast cooldown with gradient  $\Delta T = 13.7$  K in 20 mG external magnetic field expels flux at  $B_{SC}/B_{NC} = 1.63$ .

By not following the fast cooldown procedure, normal conducting vortices may get trapped within the superconducting lattice. Oscillation of vortices during RF operation introduces significant dissipation [11, 12]. If all regions reach  $T_c$  simultaneously, the superconducting phase nucleates in multiple locations [7, 8]. If attraction between vortices and pinning sites is more energetically favorable than the onset of superconductivity, flux becomes trapped, and we observe minimal change in the magnetic field [9], like in Fig. 2.

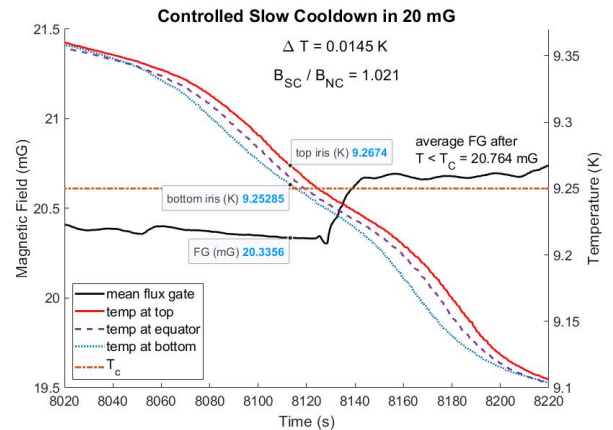


Figure 2: Slow cooldown with gradient  $\Delta T = 0.0145$  K in 20 mG external magnetic field traps flux at  $B_{SC}/B_{NC} = 1.021$ .

For accelerator application, we need SRF cavities to be robust against small magnetic fields, as creating a large thermal gradient across many cryomodules is difficult. For cavities with poor flux expulsion, we must fix this issue in order to reach high  $Q_0$ . A high temperature anneal of 900 °C or 1000 °C is known to improve flux expulsion [6, 9, 13–17]. Alongside this improvement, sample studies observe grain

growth and changes in grain orientation [6, 13, 15, 18]. Flux pinning is related to defects in the crystal structure which motivates materials studies to make this connection [19, 20].

The success of intentionally added impurities to the niobium surface has drawn deeper questions about how these impurities affect cavity behavior, and has prompted an investigation of cavities with a low residual resistance ratio (RRR). Low purity niobium has been studied previously for the purpose of cost reduction and possible high  $Q_0$  [21]. In this study, we view intrinsic impurities as a resource to understand the mechanism of impurity-based improvements.

In our low RRR cavity, flux is nearly fully trapped at all thermal gradients, even after 1000 °C annealing [22]. We ask why this is not enough to resolve the problems of low RRR material. Low RRR niobium has a higher concentration of impurities and defects, which would serve as pinning sites for higher sensitivity to trapped flux [6]. We concentrate on the connection between flux expulsion in low RRR cavities and the crystal structure of the niobium material.

## RESULTS

We quantify flux expulsion via measurements of fluxgate magnetometers on the cavity equator while cooling down across  $T_c$  in a uniform magnetic field [9]. We take the ratio of the measured magnetic field before ( $B_{NC}$ ) and after ( $B_{SC}$ ) the superconducting transition. If flux is fully expelled, we observe  $B_{SC}/B_{NC} \approx 1.7$  [8], like in Fig. 1. If flux is fully trapped,  $B_{SC}/B_{NC} \approx 1$ , like in Fig. 2. Thermometers at the top and bottom irises measure the thermal gradient ( $\Delta T$ ) across the cavity. For different cooldowns, we plot  $B_{SC}/B_{NC}$  versus  $\Delta T$  in Fig. 3 to understand the efficiency of flux expulsion. The key result of this study is that the low RRR cavity achieves full flux expulsion after 1200 °C annealing.

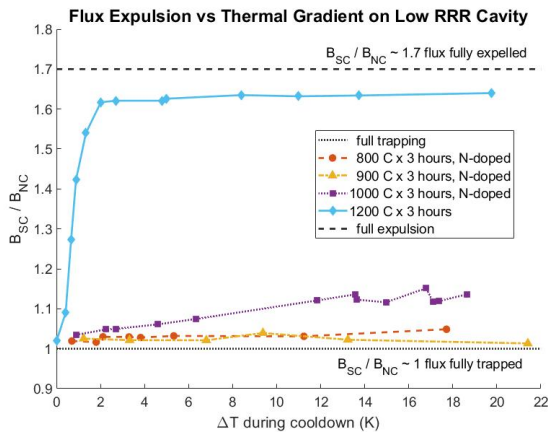


Figure 3: Flux expulsion ratio vs thermal gradient plotted for different heat treatments.

We conduct a sample study using low RRR coupons cut from the same sheet as the cavity to correlate the RF behavior with the material properties. Through secondary ion mass spectrometry, we found no impurities which explain the dramatically lower RRR [23], so we determine crystal structure governs the RRR in this sheet. Because grain boundaries are

known to increase scattering, it is necessary to treat them as impurities in the niobium lattice [19, 24, 25]. We ask how the crystal structure responds differently to high-temperature annealing. We bake the samples from 800 °C up through 1200 °C, each for 3 hours, to observe how low RRR material responds. The results are summarized in Table 1.

Table 1: Low RRR Sample Statistics

Sample	RRR	Median Grain [ $\mu\text{m}$ ]	Grain Size (G) [26]	LAM [ $^\circ$ ]
EP only	35	14.3	8.3	0.15
800 °C	63	10.7	8.9	0.14
900 °C		19.5	7.6	0.14
1000 °C	128	22.3	7.3	0.12
1100 °C		36.8	5.3	0.10
1200 °C		136	2.2	0.08

We perform electron backscatter diffraction to observe defects at the sample surface. Images from scanning electron microscopy are processed by the AZtecCrystal software into maps of the crystal structure. A grain is defined as a region of the crystal structure showing the same crystalline orientation, with its boundary having a change in orientation. Our threshold angle for a grain boundary is 2 °. We export a list of detected grains, and plot grain size as the square root of the grain area, in Fig. 4. While we observe significant increase in the RRR between as received condition and 1000 °C, we don't observe major grain growth until 1200 °C.

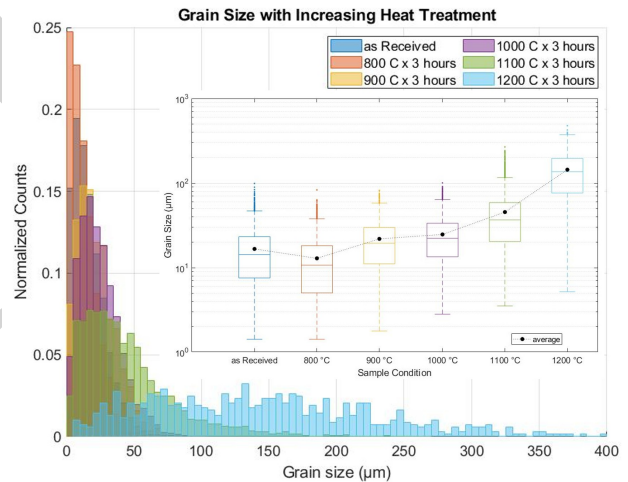


Figure 4: Histogram and box plots of grain size for different heat treatments.

We export the detected euler angles for each pixel. From this, we calculate the crystal orientation with respect to the surface normal direction. The distribution of orientations is plotted as inverse pole figures in Fig. 5, where red represents a larger proportion of the pixels. From 800 °C up through 1100 °C, we observe a preference toward both the 100 and 111 directions. Only at 1200 °C does the preference shift entirely toward 111.

We export local average misorientation (LAM) for each pixel, plotted in Fig. 6. This is the deviation in orientation

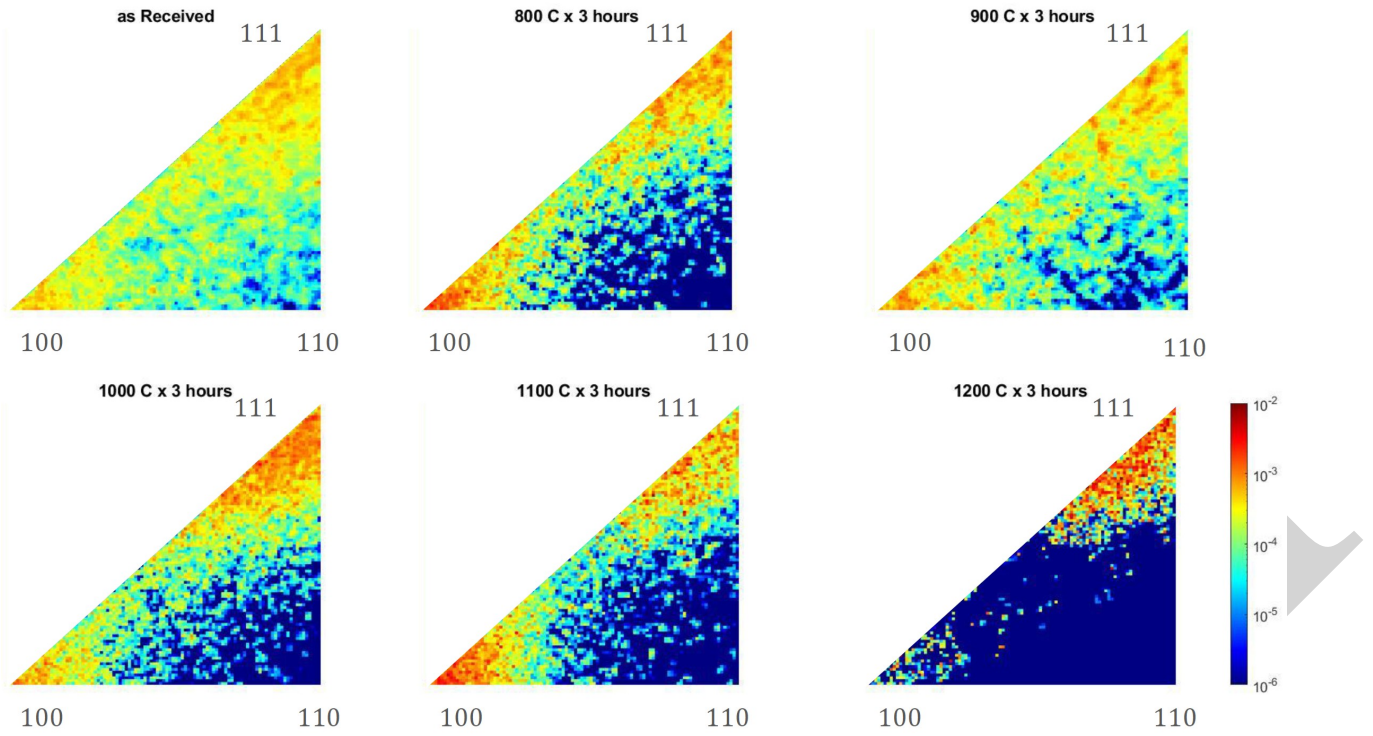


Figure 5: Inverse pole figures show the evolution of the crystal orientation for different heat treatments.

from the grain’s average orientation, and is a measure of the dislocations within the lattice. For increasing temperature, we observe a steady decrease in LAM.

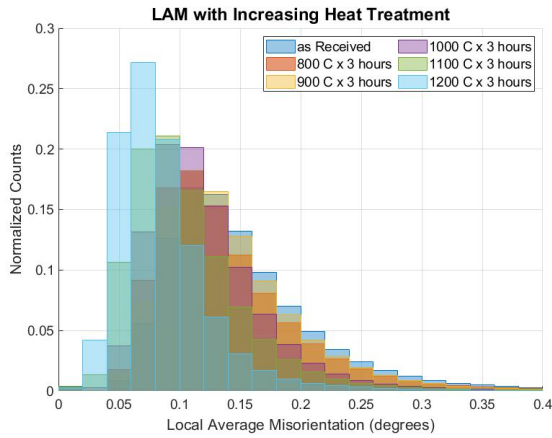


Figure 6: Histogram of local average misorientation for different heat treatments.

## CONCLUSION

In this study, we achieve flux expulsion in the low RRR cavity after 1200 °C annealing. We observe grain growth, shift in orientation, and decreasing LAM with increasing temperature. We identify parameters that change between 1000 °C and 1200 °C that may explain this improvement. The small grain size after 1000 °C annealing is a possible explanation of why this was not enough to expel flux.

Below 1200 °C, we observe preference in grain orientation toward 100 and 111. The preference consolidates toward

111 at 1200 °C, alongside improved flux expulsion. Other studies have correlated recrystallization and improved RF performance with this shift [25,27]. The observed decrease in misorientation has also corresponded to improved RF performance [19,24]. Grain recovery that occurs at lower annealing temperature leaves behind flux-trapping defects in the superconducting lattice [29]. The low RRR material in this study required higher annealing temperature to achieve full recrystallization and flux expulsion, in agreement with previous work [14,28,29].

For cavities with poor expulsion, sample studies on the could identify what temperature is enough to recrystallize without going over. Understanding the required parameters for good flux expulsion will provide input on vendor specifications for what material is acceptable for cavity fabrication.

## ACKNOWLEDGMENTS

This manuscript has been authored by FermiForward Discovery Group, LLC under Contract No. 89243024CSC000002 with the U.S. Department of Energy, Office of Science, Office of High Energy Physics. This work was supported by the University of Chicago and completed entirely without the use of generative AI tools.

## REFERENCES

- [1] S. Belomestnykh and S. Posen *et al.*, "Key directions for research and development of superconducting radio frequency cavities", in *Proc. Snowmass 2021*, 2022. [doi:10.48550/arXiv.2204.01178](https://doi.org/10.48550/arXiv.2204.01178)

- [2] P. Dhakal, "Nitrogen doping and infusion in SRF cavities: A review", *Phys. Open*, vol. 5, p. 100034, 2020. doi:10.1016/j.physo.2020.100034
- [3] D. Gonnella, J. Kaufman, and M. Liepe, "Impact of nitrogen doping of niobium superconducting cavities on the sensitivity of surface resistance to trapped magnetic flux" *J. Appl. Phys.*, vol. 119, no. 7, p. 073904, 2016. doi:10.1063/1.4941944
- [4] M. Checchin *et al.*, "Frequency dependence of trapped flux sensitivity in SRF cavities", *Appl. Phys. Lett.* vol. 112, p. 072601, 2018. doi:10.1063/1.5016525
- [5] D. Gonnella *et al.*, "Nitrogen-doped 9-cell cavity performance in a test cryomodule for LCLS-II", *J. Appl. Phys.*, vol. 117, p. 023908, 2015. doi:10.1063/1.4905681
- [6] P. Dhakal, G. Ciovati, and A. Gurevich, "Flux expulsion in niobium superconducting radio-frequency cavities of different purity and essential contributions to the flux sensitivity", *Phys. Rev. Accel. Beams*, vol. 23, p. 023102, 2020. doi:10.1103/PhysRevAccelBeams.23.023102
- [7] T. Kubo, "Flux trapping in superconducting accelerating cavities during cooling down with a spatial temperature gradient", *Prog. Theor. Exp. Phys.*, vol. 2016, p. 053G01, 2016. doi:10.1093/ptep/ptw049
- [8] A. Romanenko *et al.*, "Dependence of the residual surface resistance of superconducting radio frequency cavities on the cooling dynamics around  $T_c$ ", *J. Appl. Phys.*, vol. 115, p. 184903, 2014. doi:10.1063/1.4875655
- [9] S. Posen *et al.*, "Efficient expulsion of magnetic flux in superconducting radiofrequency cavities for high Q applications", *J. Appl. Phys.*, vol. 119, no. 21, p. 213903, 2016. doi:10.1063/1.4953087
- [10] S. Huang, T. Kubo, and R. L. Geng, "Dependence of trapped-flux-induced surface resistance of a large-grain Nb superconducting radio-frequency cavity on spatial temperature gradient during cooldown through  $T_c$ ", *Phys. Rev. Accel. Beams*, vol. 19, no. 8, p. 082001, 2016. doi:10.1103/PhysRevAccelBeams.19.082001
- [11] M. Checchin *et al.*, "Electron mean free path dependence of the vortex surface impedance", *Supercond. Sci. Technol.*, vol. 30, p. 034003, 2017. doi:10.1088/1361-6668/aa5297
- [12] M. Martinello *et al.*, "Effect of interstitial impurities on the field dependent microwave surface resistance of niobium", *Appl. Phys. Lett.*, vol. 109, p. 062601, 2016. doi:10.1063/1.4960801
- [13] A. D. Palczewskiet *et al.*, "Study of Flux Trapping Variability between Batches of Tokyo Denkai Niobium used for the LCLS-II Project and Subsequent 9-cell RF Loss Distribution between the Batches", in *Proc. SRF'19*, Dresden, Germany, Jun.-Jul. 2019, pp. 570–575. doi:10.18429/JACoW-SRF2019-TUP057
- [14] G. R. Myneni *et al.*, "Medium grain niobium SRF cavity production technology for science frontiers and accelerator applications", *J. Instrum.*, vol. 18, p. T04005, Apr. 2023. doi:10.1088/1748-0221/18/04/T04005
- [15] Z. Sung *et al.*, "Evaluation of predictive correlation between flux expulsion and grain growth for superconducting radio frequency cavities", *Supercond. Sci. Technol.*, vol. 36, no. 9, p. 095015, Jul. 2023. doi:10.1088/1361-6668/ace4fb
- [16] B. Khanal and P. Dhakal, "Evaluation of Flux Expulsion and Flux Trapping Sensitivity of SRF Cavities Fabricated from Cold Work Nb Sheet with Successive Heat Treatment", in *Proc. SRF'23*, Grand Rapids, MI, USA, Jun. 2023, pp. 197–201. doi:10.18429/JACoW-SRF2023-MOPMB042
- [17] B. D. Khanal *et al.*, "Role of microstructure on flux expulsion of superconducting radio frequency cavities", *Supercond. Sci. Technol.*, vol. 38 p. 015015, 2025. doi:10.1088/1361-6668/ad9ad7
- [18] H. Umezawa *et al.*, "Relationship between anisotropy and cross rolling process for high purity niobium sheets", in *Proc. IPAC'24*, Nashville, TN, May 2024, pp. 3893–3896. doi:10.18429/JACoW-IPAC2024-THPS63
- [19] C. Z. Antoine, "Influence of crystalline structure on rf dissipation in superconducting niobium", *Phys. Rev. Accel. Beams*, vol. 22, p. 034801, 2019. doi:10.1103/PhysRevAccelBeams.22.034801
- [20] S. Balachandran *et al.*, "Direct evidence of microstructure dependence of magnetic flux trapping in niobium", *Sci Rep*, vol. 11, p. 5364, 2021. doi:10.1038/s41598-021-84498-x
- [21] G. Ciovati, P. Dhakal, and G. R. Myneni, "Superconducting radio-frequency cavities made from medium and low-purity niobium ingots", *Supercond. Sci. Technol.*, vol. 29, no. 6, p. 064002, 2016. doi:10.1088/0953-2048/29/6/064002
- [22] S. Posen, private communication, Apr. 2024.
- [23] K. Howard *et al.*, "Microscopic understanding of the effects of impurities in low RRR SRF cavities", in *Proc. IPAC'24*, Nashville, TN, May 2024, pp. 2829–2832. doi:10.18429/JACoW-IPAC2024-WEPS59
- [24] P. Kneisel *et al.*, "Review of ingot niobium as a material for superconducting radiofrequency accelerating cavities", *Nucl. Instrum. Methods Phys. Res., Sect. A*, vol. 774, pp. 133–150, 2015. doi:10.1016/j.nima.2014.11.083
- [25] A. Dangwal Pandey *et al.*, "Grain boundary segregation and carbide precipitation in heat treated niobium superconducting radio frequency cavities", *Appl. Phys. Lett.*, vol. 119, no. 19, p. 194102, 2021. doi:10.1063/5.0063379
- [26] *Standard Test Methods for Determining Average Grain Size Using Semiautomatic and Automatic Image Analysis*, ASTM E1382-97(2023), ASTM International, West Conshohocken, PA, 2023. doi:10.1520/E1382-97R23
- [27] T. R. Bieler *et al.*, "Physical and mechanical metallurgy of high purity Nb for accelerator cavities", *Phys. Rev. Spec. Top. Accel. Beams*, vol. 13, no. 3, 2010. doi:10.1103/physrevstab.13.031002
- [28] T. J. Bennet IV *et al.*, "Effects of Grain Size and Interstitial Content on Recrystallization in Nb after Cold Rolling", *IEEE Trans. Appl. Supercond.*, vol. 35, no. 5, pp. 1–5, Aug. 2025. doi:10.1109/TASC.2025.3538673
- [29] E. Taleff *et al.*, "Characterizing and controlling recovery and recrystallization in niobium for improved SRF cavity performance", in *Proc. SRF2025*, Tokyo, Sep. 2025, pp. 675–680. doi:10.18429/JACoW-SRF2025-THP34